PCCP

Accepted Manuscript

ROYAL SOCIETY OF CHEMISTRY

www.rsc.org/pccp

Stability and Binding Interaction of Bilirubin on Gold Nano-surface: Steady State Fluorescence and FT-IR Investigation

Mritunjoy Maity, Supriya Das and Nakul C Maiti*

Division of Structural Biology and Bioinformatics; CSIR-Indian Institute of Chemical Biology; 4, Raja S.C. Mullick Road, Kolkata, India-700032;
Fax: (+) 91 33 24735197, 91 33 24723967; Tel: (+) 91 33 24995940

Received date:

* Address correspondence to Nakul C. Maiti, Division of Structural Biology and Bioinformatics, CSIR-Indian Institute of Chemical Biology, 4, Raja S.C. Mullick Road, Kolkata 700032

E-mail: ncmaiti@iicb.res.in

Phone: +91-33-2499-5940, +91-33-2473-5197/2472-3967

ABSTRACT

Gold nanoparticle exhibits strong absorption and emission due to its unique physical geometry and surface plasmon resonance phenomena. A further modification with organic molecules makes it more appropriate for biological applications. The current manuscript illustrated optical behavior and stability of bilirubin (BR) coated gold nanoperticles (AuBR), using BR itself as a reducing agent. In addition, FT-IR and steady state fluorescence measurements were performed to illustrate the binding interaction of BR with Au (III) ion and the nanoparticles. BR showed a strong affinity towards Au (III) and the measured binding constant was ~4.3 X 10^5 M^{-1}. It caused reduction of Au (III) ion and rendered the formation of cubic face centered AuBR nanoparticles which was ~20 nm in diameter. The particles were stabilized as BR bound to the gold surface and it was confirmed by FT-IR measurement. An intense carboxyl C=O stretching vibration at 1695 cm^{-1} was observed in BR powder and it was absent in AuBR. However, two weak bands at ~ 1563 and 1391 cm^{-1}, presumably due to the asymmetric and symmetric stretching vibration of the carboxylate form (COO^-), were found in AuBR. Stretching vibration of the lactam C=O appeared at 1645 cm^{-1} in BR and the band was shifted to 1647 cm^{-1} in AuBR. The stretching modes of the pyrrole N–H and the lactam N–H were detected at 3406 cm^{-1} and 3267 cm^{-1}, respectively, in BR. However, the pyrrole N–H band shifted to 3446 cm^{-1}, and became broader in AuBR. The observed blue shift in the lactam C=O and the N–H vibrations in AuBR indicated weakening/absence of internal hydrogen bonds between carboxyl groups and the four N–H bonds in the BR moiety. The binding of BR to the surface provides great stability to the nanoparticles and it remained monodispersed in the large pH range (pH 4 to 12) for more than a month. However, in acidic pH the particles associated to form bigger particle and the plasmon resonance band shifted as they grew; plasmon resonance band

shifted from 525 nm (at pH 7.0) to 555 nm (at pH 3.0). The particles also remained stable in the presence of higher concentration of salt (KCl and NaCl) in the dispersing media.

Keywords

nanoparticles, hydrogen bond, plasmon, gold, monodispersed.

Introduction

Due to unique size, shape and special electrochemical behaviour, gold nanoparticles (AuNP) exhibit unique optical features such as surface plasmon resonance that gives rise to a sharp and intense absorption band in the visible range.[1-3] Surface plasmon resonance is happened due to collective resonant oscillation of free electrons of the conduction band of the metal. It causes an intense optical extinction and depends on content of free electrons on the metal surface and the dielectric properties of the local medium. This prominent spectroscopic feature and size make nanoparticles very useful and functional in several fields such as catalysis,[4] biotechnology,[5] in making electronic devices[6] and medicine.[7] Several reports further indicated application of AuNP as antibacterial and antiviral reagent,[8, 9] in cancer cell imaging,[10-13] photothermal therapy,[5, 14, 15] drug delivery.[16-20] In addition, the nanocomposites of organic dye molecules and nanoparticles showed high impact in biosensing and related fields.[21-24] It is very attractive to use in bio-imaging, medicine and technology because of its chemical stability and unique propensity to bind thiol (-SH) group of proteins and similar other targets.[25] To be used in different field, evolution in the synthesis and defining stability and optical sensitivity of gold nanoparticles continue with many reagents and proposed several solution condition.

A common method for production of gold nanoparticles using typical chemical reduction methods including the classical Turkevich citrate reduction method[26, 27] and some modification are done using variety of organic solvents.[28-30] In these procedures, typically, $HAuCl_4$ is reduced by citric acid which simultaneously functions as a stabilizing agent [31] or is reduced by $NaBH_4$ in the presence of thiol or carboxylic acid stabilizers.[32] Sometimes pernicious and highly volatile organic solvents are used as the

reaction medium such as hydrazine hydrate reduction,[33] polyol process and modified polyol process,[34, 35] photochemical reduction,[36, 37] electrochemical reduction,[38] microwave induction.[39] Most of these processes are employed through wet chemistry methods with the use of highly reactive inorganic reducing agents such as $NaBH_4$, hydrazine hydrate (N_2H_4, H_2O) etc. which are not eco-friendly. To avoid toxic reagents, eco-friendly solvent like water and biological materials as capping/stabilizing reagents have been used in these synthesis methods. Reports include use of amino acids,[40] vitamins,[41] use of plant extracts,[42] and other environmentally benign biological compounds as reducing agents [43] to exclude the use of toxic reagents.

In the current manuscript we have presented a study to show synthesis of gold nanoparticle using bilirubin (BR) as both the reducing agent and stabilizing molecule. Further we have illustrated the binding interaction of adsorbed bilirubin on the gold nano surface and formation of BR stabilized gold nanoparticle (AuBR). Formation of BR assisted preparation of gold nanoparticles was reported,[44] however, no other detail investigation regarding stability, reduction mechanism and binding interaction was investigated. The current manuscript has detailed the affinity of Au (III) ion towards BR, the mechanism of reduction of gold ion to produce nanoparticle, the role of BR in stabilizing the nanoparticles and its binding interaction and structure on the surface of gold nanoparticles.

The structure of BR on nano-surface may be a key factor in understanding nanoparticle formation and stabilization. FT-IR is an effective technique to investigate the interaction between metal surface and the bound molecule.[31, 45-49] Changes in vibrational frequencies and the variation in intensities in the spectra of adsorbed molecules compared to that in free provide information on relative interaction and binding stability of the ligand. FT-IR study confirmed that the intramolecular hydrogen bonds of BR

broke out and carboxyl group ionized and remained bound to the metal surface. The bound BR facilitated the particle to gain extraordinary stability and monodispersity in aqueous solution.

Experimental Details

Materials and Methods

All chemicals used were of analytical grade or of the highest purity available. Hydrogen tetrachloroaurate (III) hydrate ($HAuCl_4.3H_2O$, 99.9%), bilirubin ($C_{33}H_{36}N_4O_6$, >98%) were purchased from Sigma-Aldrich. Sodium hydroxide (NaOH) was purchased from Merck Millipore. All reagents were used as received. Glassware was carefully cleaned with aqua regia (3:1 HCl/HNO_3), and then rinsed several times with Mill-Q (18 MΩ.cm resistance at 25 ^oC) water prior to use under sonication. Mill-Q water was used to prepare all the solutions in this study.

Absorption spectroscopy

Absorption spectra of prepared gold nanoparticles were measured with a JASCO V-630 Spectrophotometer (JASCO International Co. Ltd, Japan) in the range of 400 to 800 nm wavelength. High quality quartz cuvette was used to record the spectra.

Transmission electron microscopy

The size of the nanoparticles was studied using transmission electron microscope (TEM). For TEM imaging, a drop of aqueous suspension of the nanoparticle solution was placed on carbon coated 300-mesh copper grid (Allied Scientific Product, USA) and dried in a dust free atmosphere. The bright field electron micrographs of the samples were taken on a Tecnai G2 Spirit Biotwin (Type: FP5018/40) at an acceleration voltage of 80 kV.

FT-IR measurement

The FT-IR spectra of the samples were recorded on a Bruker TENSOR27 spectrometer using the KBr pellet technique. Solid samples (bilirubin/AuBR) were mixed with KBr in a clean glass pestle and mortar and compressed to obtain a pellet. The spectra were recorded from 400–4000 cm^{-1}. Background spectra were obtained with a KBr pellet for each sample. Bruker software was used for data processing. The strong peaks in the spectra were reproducible and appeared each time within ± 3 cm^{-1}.

Fluorescence measurement

The Intrinsic fluorescence measurements of bilirubin were recorded on Agilent Technology, Cary Eclipse fluorescence spectrophotometer. The excitation wavelengths and emission measurement were selected according to the sample, with fixed excitation and emission slit widths of 5 nm each. The quartz cuvette (4 cm × 1 cm × 1 cm) with path length of 1 cm was used. All the experiments were carried out at room temperature (24^{o}C).

For fluorescence quenching measurements, the intrinsic fluorescence of BR was measured in the presence and in the absence of Au (III). The fluorescence of BR was found to quench in the presence of Au (III). The quenching experiment was carried out simply by adding 2.5 μL aliquot (stock solution of gold salt 1.6 mM) solution to 2 mL BR. Small error due to dilution upon addition of the gold salt was neglected. Gold salt showed negligible absorbance at the excitation wavelength (470 nm) compared to BR absorption at this wavelength. Fluorescence intensities at 520 nm were recorded as a function of Au (III) concentration. To derive the binding parameters, obtained data were analyzed using modified Stern–Volmer equation.[50]

Synthesis of Gold nanoparticles

Au (III) solution was prepared by dissolving required amount of hydrogen tetrachloro aurate (III) hydrate solution in the Mili-Q water in a 100 ml clean round bottle flask and adjusted the pH ~7 of the solution by the addition of aqueous 0.25M NaOH solution. Separately, bilirubin solution was prepared by dissolving required amount of bilirubin in Milli-Q water at pH ~8 in another clean round bottle flask covered with aluminium foil.[51] Bilirubin solution was added slowly to the Au (III) solution with vigorous stirring at 1200 rpm under dim room light condition. Subsequently, to the reaction mixture 0.5M NaOH solution was added drop wise to raise the pH to 9.0. The final concentrations of both Au (III) and bilirubin in the reaction medium were 0.25mM and molar ratio of Au (III) /bilirubin was 1:1. The stirring was continued for additional few hours. The reaction mixture subsequently was centrifuged at 18000 rpm for 15 min. The collected gold nanoparticle (AuBR) was pinkish red in color.

To examine the effect of pH on the production rate of AuBR experiment was also perform at higher pH. It was observed that with the increase of pH in the reaction mixture, rate of the particle formation increased and the completion time of the reaction was decreased. Keeping the concentration of starting materials same, approximate reaction time at pH 9, 10 and 12 were about 18 h, 15 h and 6 h, respectively. To wash the nanoparticles, the produced material was re-dispersed in deionized water and centrifuged. The process was repeated for three times to remove excess bilirubin and other by-products. This purified AuNPs was used for further investigation.

Results

The UV-visible spectrum of gold nanoparticles prepared at pH 9.0 and dispersed in water is shown in Figure 1A. The band maxima appeared at ~525 nm which is due to the surface plasmon resonance (SPR) effect of gold nanoparticles. The peak position and shape of the band was related to the particle size. Relatively clean band at 525 nm indicated the average particle size ~ 20 nm in diameter.[52, 53] AuNP was also prepared at three other pH conditions and the suspended particles in all cases showed similar plasmon resonance band at ~ 525 nm indicating that pH of the reaction mixture did not affect much on the shape and size of the produced nanoparticles. However, the rate of nanoparticle formation was pH dependent (discussed in preparation section).

Figure 2 inset shows the XRD spectrum of the synthesized gold nanoparticles. The joint committee on powder diffraction standards Card no. 03-065-2870 of pure crystalline gold structures was used to define the crystalline nature of the gold particle. A comparison of the XRD spectrum confirmed that the synthesized gold nanoparticles were in the form of face-centered cubic nanocrystals with Fm3m symmetry, as evidenced by 2θ values 38.27°, 44.33°, 64.92°, and 77.59° in the XRD pattern, corresponding to (111), (200), (220), and (311) planes, respectively.

A TEM image of AuBR prepared at pH 9 is shown in figure 2. The particles produced under basic conditions (pH 9.0, 10.0 and 12.0) were spheroidal and mono-dispersed. The average diameter of the nanoparticles was ~ 20 nm as confirmed by the TEM images. Plasmon resonance band that appeared at 525 nm also indicated that the average size of the particles was ~ 20 nm.[52, 53]

Binding affinity of BR to Au (III): fluorescence study

The binding affinity of Au (III) for BR at pH 9.0 was measured by measuring the intrinsic fluorescence of BR in the presence of different concentration of the gold salt. BR showed a strong fluorescence with an emission peak at 530 nm. The addition of Au (III) to a BR solution led to reduction in the fluorescence intensity and gradual decrease with increase of the Au (III) ion concentration (Figure 3A).

To determine the binding parameter, the fluorescence data obtained in the above experiments were analyzed using a modified S–V equation (Equation 1) (Lakowicz 2006, 3rd edition, p. 289).[50] Fluorescence intensity at 520 nm of the BR solution at different concentration of Au (III) was fitted to the equation and the plot is shown in Figure 3B.

$$F_0/\Delta F = 1/(f\,K\,[Q]) + 1/f \quad \text{..... (1)}$$

Where F_0 is the initial fluorescence intensity in the absence of Au (III), ΔF is the difference in fluorescence in the absence and presence of the Au (III) at concentration [Q], K is the S–V quenching constant, and f is the fraction of the initial fluorescence which is accessible to the quencher.[50] The plots of $F_0/\Delta F$ versus 1/[Q] yield f^{-1} as the intercept, and $(f\,K)^{-1}$ as the slope. The S–V quenching constant as obtained from the modified S–V equation can be expressed as binding affinity constant, K_a.[50, 54-56] The reciprocal of K_a gives the dissociation constant, K_d, was found to be 2.3 μM. The value of K_a was $4.3 \times 10^5\ M^{-1}$.

The intercept on y axis ($f^{-1} = 1$) indicated that ~100% of the total BR fluorescence was accessible for the Au (III).[50, 54-56] This fact indicated that the fluorescence quenching of BR solution by Au (III) was dominated by static quenching mechanism. Quenching of

fluorescence requires close proximity between the quencher and fluorophore (BR). Depending on the chemical structure, property and its interaction, generally two types of quenching may occur: dynamic and static quenching.[50] In dynamic quenching, the quencher needs to diffuse to the fluorophore during its excited state lifetime. In some cases excited state energy transfer also occurs from the fluorophore to the quencher molecule via long range dipole-dipole interaction.[50, 57, 58] As the dynamic fluorescence quenching processes is primarily via a collisional process, solvent viscosity and size of the particles play vital roles on the extent of quenching. During dynamic quenching both the intrinsic physical and chemical properties of the fluorophore and the quencher remain unchanged.[57, 59] In static quenching, hydrophobic and electrostatic interactions between the fluorophore and the quencher lead to the formation of a non-fluorescent ground state complex (dark complex) with different physicochemical properties. [50, 54, 55, 57] In the static process, due to a close association of the fluorophore and the quencher often causes substantial loss of fluorescence. Addition of Au (III) to BR solution led to a significant reduction in the fluorescent intensity of BR compared to its initial fluorescence without the gold ion as shown in Figure 3A. Fluorescence quenching of BR in the presence of Au (III) followed the static modes as the f^{-1} value was close to 1 (Eq. 1) and strongly suggested static quenching.

To gather additional support for the proposed static quenching mechanism, the absorption spectrum of BR was monitored in the presence of different concentration of Au (III) as shown in Figure S2. It is apparent that the absorption peak of BR gradually decreased as the amount of Au (III) increases. Such a major change in absorption indicated that in the presence of Au (III) ion, BR changed and might bind and form a ground state complex (that eventually produced the nanoparticle). Thus the modified Stern-Volmer plot and absorption study clearly indicated that fluorescence quenching of

BR by Au (III) happened due to formation of a static type ground state complex formation.

Reduction of Au (III) by bilirubin

The binding of bilirubin (BR) to Au (III) and subsequent reduction of this ion is crucial for the formation of nano structure. So far no detail reduction mechanism of the metal ion by BR has been established. To start the reaction the aqueous solution of bilirubin was added drop wise to the Au (III) solution. In the beginning the solution transformed to blackish green from golden yellow color, indicating the reduction of Au (III) to Au (0) and formation of very small particles. Afterwards, a significant color change was observed by vigorous stirring; then the solution turned deep red and indicated formation of nanoparticles of bigger size (~20 nm). The reaction mixture was kept in stirring condition and dropwise NaOH solution (0.5 M) was added to keep the pH of reaction mixture constant. After 30 min, the color of the reaction mixture turned to reddish green and the appearance of this color indicated the formation of gold nanoparticles and the reaction was finished as per time mentioned below. As the pH of the solution and ionic environment of the reaction media play an important role in the nucleation process of gold atom from Au (III) state, the reaction was carried out at several pH conditions to establish the reaction mechanism. The formation rate of gold nanoparticle (AuNP) at pH 7.0, room temperature, was slow. Upon addition of NaOH solution, the reduction of $HAuCl_4$ by bilirubin was increased. At pH 9.0, the completion of the reaction took about 24 hours and however, it became quite fast at pH 12 and the reaction was completed in ~ 6 hours. However, at the lower pH (~ 6.1), the color of the solution did not change within 24h, indicating that the reduction was not completed, and no plasmon resonance band was observed.

We propose here a possible mechanism for the reduction of Au (III) by bilirubin in basic condition. The usual chemical structure of bilirubin (alpha form) is showed in **Figure 4A** and the structure is not planar, rather involutes intramolecular hydrogen bond formation which provides stability to the molecule. It consists of four pyrrole rings, two carbonyl groups and two carboxyl groups. The intramolecular hydrogen bond shields the hydrophilic sites of the bilirubin molecule and render it weakly soluble in water. However, in alkaline pH, solubility increased due to ionization of the COOH group. The reduction of Au (III) may be the direct hydrogen abstraction induced by the metal ion from bridge methylene in basic condition and this process may increase with the increase of OH^- ion concentration. As shown in the scheme 1. Another possible way could be the reduction of metal precursor by the organic radicals formed in reaction medium.

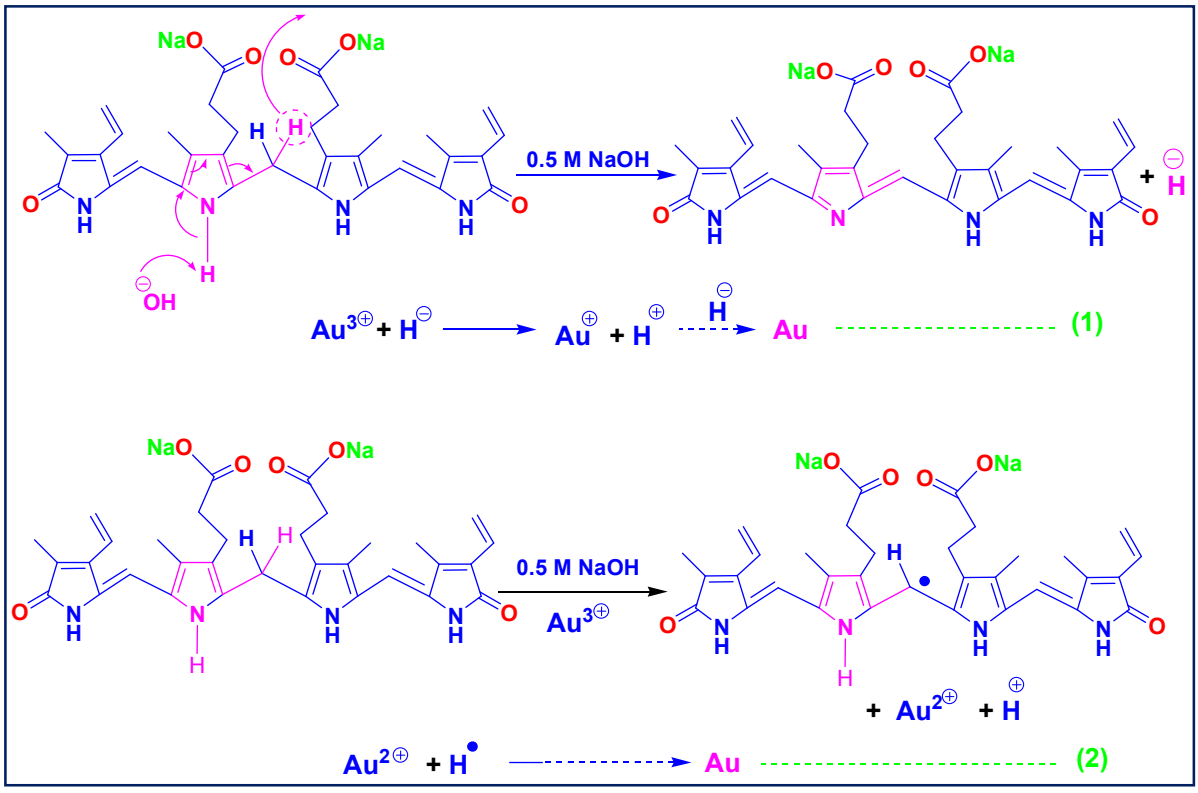

Scheme 1: Reduction mechanism of Au (III) to Au (0) by bilirubin in alkaline pH.

Fluorescence emission of AuBR

The fluorescence and adsorption studies of BR and AuBR in aqueous buffer solution were carried out further to realize surface adsorption of BR. Figure S1, panel A shows the absorption spectrum of free bilirubin (BR) in phosphate-buffer, a broad absorption peak appeared at ~ 440 nm. AuBR in similar buffer condition showed very broad and weak absorption where free BR absorbed indicating adsorption of the BR molecules on the nanoparticles surface. However, the characteristic plasmon absorption band of the nanoparticles was present at 520 nm. A bleaching/attenuation of absorption of molecules adsorbed on nanosurface is often observed and it is explained based on different interrelated electromagnetic interaction on metal surface.[60] This kind of changes in optical behavior, otherwise, confirms the association/adsorption of organic molecules on the metal surface.

AuBR with largely attenuated absorption peak (due to surface attached BR) showed fluorescence with a peak position at ~578 nm (Figure S1, panel D). The fluorescence spectrum was relatively broad and red shifted compared to the fluorescence band of BR in similar solution condition (Figure S1, panel B). The red shift and broadness of the fluorescence, an expected manifestation of combined electromagnetic interaction of the adsorbed molecule on/near metal nanosurface,[60] further indicated the strong association of BR with the surface of gold nanoparticles.

Bonding and interaction pattern of BR on gold nanosurface

The FT-IR spectra of bilirubin and AuBR are shown in Figures 5A and 5B**,** respectively. In addition to the bands in the 600-1700-cm^{-1}, the spectra show bands at high frequency region (2850-3450 cm^{-1}). The significant FT-IR bands of both BR powder and AuBR and their assignments were summarized in Table 1. Some of the characteristic FT-IR bands of strong and medium intensity appeared at 3406, 3267, 2912, 1695, 1645, 1611,

1250, 989 and 932 cm^{-1} and, other bands at 800-600 cm^{-1} were marked in the spectra. The bands were very consistent with the normal mode analysis of vibration frequency of BR[61] and the assignments were made following the literature values.[61-63]

Based on the normal coordinate analysis data[61-63], the 3406 and 3267 cm^{-1} bands observed in BR powder were assigned to the stretching modes of the pyrrole N–H and the lactam N–H, respectively. Pyrrole N–H shifted to 3446 cm^{-1} and became broader on the nano surface. Asymmetric lactam N–H stretching frequency of BR on gold nano surface appeared as shoulder in a broad band of pyrrole N–H. Similarly, asymmetric CH_2 stretching vibration at 2912 cm^{-1} of BR weakly appeared at 2915 cm^{-1} in AuBR. 1188 cm^{-1} band was assigned to pyrrole ring breathing mode and it was very weak in AuBR and might be shifted to 1165 cm^{-1} due to surface association of bilirubin with the gold nanoparticles.

BR contains two carboxyl side chains and produced intense carboxyl C=O stretching vibration at 1695 cm^{-1}. However, this band was absent in BR bound to the nanosurface (AuBR). Two weak bands were observed at ~ 1563 and 1391 cm^{-1} and assigned to the asymmetric and symmetric stretching vibration of the carboxylate form (COO^-) of BR attached to gold nanoparticle. 1645 cm^{-1} band was assigned to lactam C=O vibration which was shifted to 1647 cm^{-1} on the nanosurface. The band at 1611 cm^{-1} was assigned to the C=C stretching of the conjugated system present in BR. The band was broadened out in AuBR. The bands at 1250, 989, and 932 cm^{-1} from the BR powder, were associated with the lactam systems (C–C, C–N vibrations) and they were broadened in AuBR. An interaction of carboxylate bound to the nano-surface could interact with water molecules adsorbed on the surface. H_2O molecules complexed with

COO^- often produce broad ν_{O-H} band at 3550−3414 cm^{-1}.[64] The observed broad FT-IR in this region could be due to the presence of moisture in the AuBR powder.

Stability of AuBR

Thermal stability of the nanoparticles in aqueous suspension was measured following the plasmon resonance band in different solution condition. BR coated gold nanoparticles (AuBR) were dried and stored under vacuum for weeks/months. Figure 1B shows the plasmon peaks in water suspension of AuBR which was stored under vacuum for different interval of time. Close inspection of the Plasmon resonance absorption band indicated very small red shift (~3 nm) due to aging for couple of months. Also scattering level was not enhanced to a large extent. These indicated that AuBR was very stable under dry condition. In wet condition also the particles showed substantial stability and remained stable for days without much perturbation in the plasmon resonance band. The particles remained stable in aqueous solution (pH 7) for 120 days at 20 ^oC and the UV-Vis optical band remained at 525 nm. Further stability test was performed in the presence of KCl and NaCl and it was observed that very high concentration (~0.8 M) of these salts had no significant effect on the stability and dispersity of the nanoparticles. Figure 1C and 1D showed that the plasmon resonance band was not broadened or increased in absorbance, suggesting their great stability in the salt solution.

Further experiment was performed to test the stability of the particles in different pH conditions. Figure 6 presents the plasmon resonance band and color of the nanoparticles suspension in acidic and basic conditions. Freshly prepared gold nanoparticle was dispersed in 10 mM phosphate buffer and the pH of the solution was varied from 3.0 to 12.0. The UV-Vis spectrum of the solution was taken after 30 minute incubation. The

Plasmon resonance band appeared at 525 nm and no detectable shift in the position could be observed in pH range of 5.0-12.0. The solution color at this pH range was remained pinkish red. These observation indicated uniformity in solution state dispersity and stability of the particles in the above pH ranges.

The solution color of the dispersed nanoparticles, however, started to become wine (deep) red at pH below 5.0. (Figure 6). The plasmon resonance band was shifted to longer wavelength (red shift) and the band maxima appeared at ~555 nm at pH 3 after 15 min of incubation. A large red shift in plasmon absorption spectra is due to formation of larger particle or the aggregation of the nanoparticles. The calculated particle sizes are mentioned in the figure. The largest size was ~ 80 nm at pH 3.0. It was possible that bilirubin attached on gold nanosurface may promote coagulation of the particles. At low pH, acidic moiety of the BR might tend to be protonated and could have strong tendency to be released from the nanosurface. Bare nanoparticles are more prone to form aggregates.[65] Bigger particles showed red shift or low energy plasmon resonance band.[32, 66] Thus the synthesized particle was quite stable at room temperature and in a moderate pH range (pH 5.0-12.0). Also the added salt to the nanoparticles solution merely affect the monodispersity of the particles in this pH range and further indicated strong bonding between gold nano surface and the BR functional groups.

Discussion

Current study illustrated mechanism and easy synthesis of gold nanoparticles by bilirubin. It also provided the binding details of the adsorbed bilirubin onto the metal surfaces. Without using any inorganic reducing and capping reagents and, also avoiding use of microwave radiation, we demonstrated a single-step green synthesis of highly stable and well dispersed gold nanoparticle using bilirubin as the capping reagent. XRD analysis confirmed that the synthesized gold nanoparticles were face centred cubic nanocrystals. In the present work we prepared gold nanoparticles from $HAuCl_4$ at different pH using bilirubin (BR) which acts as a mild reducing agent. The method is environment friendly and a kind of 'green methods' and avoided use of hazardous solvent, reagents and the elimination of toxic side products.

Our investigation suggested that two important parameters of the reaction were controlled by pH: (a) the reactivity of Au (III) complexes with OH^- group, which depends on the pH of the reaction mixture and (b) the reduction ability of bilirubin by introducing NaOH. Goia et al reported that the reactivity of the Au (III) complexes with chloride and or hydroxide as the ligands reflected by their reduction potential. They found that the reactivity of Au (III) decreased upon increasing pH, owing to the lower reduction potential of $Au(OH)_4^-$ (+0.56V) compare to $AuCl_4^-$ (+1.002V).[67] It is obvious that the acceleration of reduction rate by NaOH in this system could not be attributed to the interaction between $AuCl_4^-$ and NaOH.[68, 69]

While rate of production of AuBR depend on the pH of the reaction solution, the size, shape and dispersity of the particle remained largely unchanged in neutral and alkaline pH. The absorption of BR rendered the nanoparticle to be mono dispersed and the size, shape and dispersity of the particle remained largely unchanged between pH 5 and 12. In

strong acidic condition (pH below 4.0) the nanoparticles became unstable, visible color of the dispersed particle changed from pinkish red to blue violet. The plasmon resonance band shifted from 525 nm at pH 7.0 to 555 nm at pH 3.0 indicating its coagulation to larger size particles. At low pH due to possible protonation of several N and acidic group of BR it may lose its strong affinity for the nanoparticles surface and got released to the solution and promotes coagulation to form a larger particle with a characteristic plasmon resonance band at 555 nm at pH 3.0.

The FT-IR absorption study confirmed the association of BR with the nanoparticle. Most of the BR bands in AuBR became broad, and shifted, and only could be identified in the expanded spectra (Figure 5). The carboxylic C=O stretching mode at 1695 cm^{-1} in BR was largely affected and shifted to much lower frequency. Asymmetric and a symmetric stretching vibrations for the carboxylate group often appear at 1500−1630 and 1305−1415 cm^{-1}, respectively.[70] The FT-IR spectra of the washed AuBR showed possible asymmetric COO^- stretching vibrations ($\nu_{asy}(COO^-)$) at 1563 cm^{-1}, and another peak assigned to symmetric COO^- stretching vibrations ($\nu_{sym}(COO^-)$) at 1391 cm^{-1} broad peak (Figure 5B).

For common acids the average carbonyl double bond (C=O), the stretching vibration modes appeared at ~1723 (± 20 cm^{-1}). It was observed that the acetic acid carbonyl adsorbed at 1706 cm^{-1}.[31] As carboxyl group of BR is hydrogen bonded with lactam rings the band was shifted to 1695 cm^{-1}. However, the loss of this band on gold surface was attributed to the ionization of the carboxyl group and binding to the metal surface (Figure 4). The average position of the asymmetric and symmetric vibration mode of carboxylate form (COO^-) appeared at 1580 (± 26 cm^{-1}) and 1406 (± 12 cm^{-1}). We observed the possible symmetric and asymmetric stretching frequencies at 1391 and 1563 cm^{-1} respectively. And the carbonyl C=O stretching in unionized COOH was

absent. It indicated that BR interaction with gold nanoparticle surface involved COO^- group of BR.

Stretching vibration of the lactam system C=O appeared at 1645 cm^{-1} in BR, however in the AuBR the band was shifted to high frequency (1647 cm^{-1}). In addition, the stretching modes of the pyrrole N–H and the lactam N–H appeared at 3406 cm^{-1} and 3267 cm^{-1}, respectively in free BR, however, the pyrrole N–H band shifted to 3446 cm^{-1} in AuBR. All the blue shifts mentioned above could be ascribed to the breaking of internal hydrogen bonds between two carboxyl groups and the four N–H bonds (two pyrrole and two lactam N–H bonds). The intramolecular H-bond involving various groups (pyrromethene rings and propionic acid) in BR were broken or became weaker as it binds to the gold nano surface. Figure 4 shows two similar dipyrromethene groups separated by a methylene unit and about six intramolecular hydrogen bonds between the propionic acid groups and pyrrole N-H and between the propionic acid groups and lactam C=O/N-H bonds. These hydrogen bonds provide conformational stability. Most of these hydrogen bonds were broken and the ionized COO^- strongly interacts with the gold nano surface (Figure 4B).

Conclusion

Bilirubin is a metabolic byproduct and the use of it to prepare gold nanoparticles is interesting in terms of environmental point of view; the preparation required no toxic solvents or reagents or additional capping molecules to stabilise the nanoparticles. The synthesised nanoparticles were quite stable at different pHs and in solutions with high salt concentration. The investigation further detailed the mechanism of Au (III) reduction by bilirubin and it suggested that alkaline condition helped the abstraction of methylene hydrogen of bilirubin. The FT-IR study established the encapsulation of bilirubin onto the gold nanoparticles. The surface attachment of BR may provide biocompatibility of the nanoparticles in biological systems. Thus, the produced AuBR may be very useful for therapeutic purposes upon modification with appropriate ligands.

References and notes

1. G. Schmid, *Chem. Rev.*, 1992, **92**, 1709-1727.
2. K. A. Willets and R. P. Van Duyne, *Annu. Rev. Phys. Chem.*, 2007, **58**, 267-297.
3. S. Link and M. A. El-Sayed, *Annu. Rev. Phys. Chem.*, 2003, **54**, 331-366.
4. A. Primo, A. Corma and H. Garcia, *Phys. Chem. Chem. Phys.*, 2011, **13**, 886-910.
5. J. P. Leung, S. Wu, K. C. Chou and R. Signorell, *Nanomaterials*, 2013, **3**, 86-106.
6. W.-F. Dong, G. B. Sukhorukov and H. Moehwald, *Phys. Chem. Chem. Phys.*, 2003, **5**, 3003-3012.
7. R. A. Sperling, P. Rivera Gil, F. Zhang, M. Zanella and W. J. Parak, *Chem. Soc. Rev.*, 2008, **37**, 1896-1908.
8. W. Zhang, Y. Li, J. Niu and Y. Chen, *Langmuir*, 2013, **29**, 4647-4651.
9. Y. Zhao, Y. Tian, Y. Cui, W. Liu, W. Ma and X. Jiang, *J Am Chem Soc*, 2010, **132**, 12349-12356.
10. X. Shi, S. Wang, S. Meshinchi, A. M. E. Van, X. Bi, I. Lee and J. R. Baker, Jr., *Small*, 2007, **3**, 1245-1252.
11. S. Mallidi, T. Larson, J. Tam, P. P. Joshi, A. Karpiouk, K. Sokolov and S. Emelianov, *Nano Lett.*, 2009, **9**, 2825-2831.
12. R. Hu, K.-T. Yong, I. Roy, H. Ding, S. He and P. N. Prasad, *J. Phys. Chem. C*, 2009, **113**, 2676-2684.
13. N. J. Durr, T. Larson, D. K. Smith, B. A. Korgel, K. Sokolov and A. Ben-Yakar, *Nano Lett.*, 2007, **7**, 941-945.
14. S.-M. Lee, H. J. Kim, Y.-J. Ha, Y. N. Park, S.-K. Lee, Y.-B. Park and K.-H. Yoo, *ACS Nano*, 2013, **7**, 50-57.
15. X. Huang, P. K. Jain, I. H. El-Sayed and M. A. El-Sayed, *Lasers Med Sci*, 2008, **23**, 217-228.
16. H. Park, H. Tsutsumi and H. Mihara, *Biomaterials*, 2013, **34**, 4872-4879.
17. G. F. Paciotti, L. Myer, D. Weinreich, D. Goia, N. Pavel, R. E. McLaughlin and L. Tamarkin, *Drug Deliv*, 2004, **11**, 169-183.
18. Y. Cheng, A. C. Samia, J. Li, M. E. Kenney, A. Resnick and C. Burda, *Langmuir*, 2010, **26**, 2248-2255.

19. X. Huang, P. K. Jain, I. H. El-Sayed and M. A. El-Sayed, *Nanomedicine (London, U. K.)*, 2007, **2**, 681-693.
20. M.-C. Daniel and D. Astruc, *Chem. Rev. (Washington, DC, U. S.)*, 2004, **104**, 293-346.
21. E. Dulkeith, A. C. Morteani, T. Niedereichholz, T. A. Klar, J. Feldmann, S. A. Levi, F. C. J. M. van Veggel, D. N. Reinhoudt, M. Moller and D. I. Gittins, *Phys. Rev. Lett.*, 2002, **89**, 203002/203001-203002/203004.
22. B. Dubertret, M. Calame and A. J. Libchaber, *Nat. Biotechnol.*, 2001, **19**, 365-370.
23. H. Imahori and S. Fukuzumi, *Adv. Mater. (Weinheim, Ger.)*, 2001, **13**, 1197-1199.
24. H. Imahori, M. Arimura, T. Hanada, Y. Nishimura, I. Yamazaki, Y. Sakata and S. Fukuzumi, *J. Am. Chem. Soc.*, 2001, **123**, 335-336.
25. J. Xie, Y. Zheng and J. Y. Ying, *J. Am. Chem. Soc.*, 2009, **131**, 888-889.
26. G. J. Hutchings, M. Brust and H. Schmidbaur, *Chem. Soc. Rev.*, 2008, **37**, 1759-1765.
27. P. C. S. a. J. H. John Turkevich, *Discuss. Faraday Soc.* , 1951, **11** 55-75.
28. G. Frens, *Nature (London), Phys. Sci.*, 1973, **241**, 20-22.
29. Y. Mastai and A. Gedanken, 2004.
30. M. Brust and C. J. Kiely, 2004.
31. J.-W. Park and J. S. Shumaker-Parry, *J. Am. Chem. Soc.*, 2014, **136**, 1907-1921.
32. K. S. Mayya, V. Patil and M. Sastry, *Langmuir*, 1997, **13**, 3944-3947.
33. H. S. Tajammul, M. Iqbal and M. Mazhar, *J. Nanopart. Res.*, 2009, **11**, 1383-1391.
34. F. Kim, S. Connor, H. Song, T. Kuykendall and P. Yang, *Angew. Chem., Int. Ed.*, 2004, **43**, 3673-3677.
35. M. Tsuji, M. Hashimoto, Y. Nishizawa and T. Tsuji, *Chem. Lett.*, 2003, **32**, 1114-1115.
36. K. L. McGilvray, M. R. Decan, D. Wang and J. C. Scaiano, *J. Am. Chem. Soc.*, 2006, **128**, 15980-15981.
37. S. Shanmugam, B. Viswanathan and T. K. Varadarajan, *Nanoscale Res. Lett.*, 2007, **2**, 175-183.
38. S.-J. Li, D.-H. Deng, Q. Shi and S.-R. Liu, *Microchim. Acta*, 2012, **177**, 325-331.

39. J. Gu, W. Fan, A. Shimojima and T. Okubo, *J. Solid State Chem.*, 2008, **181**, 957-963.
40. S. Si, A. Kotal and T. K. Mandal, *J. Phys. Chem. C*, 2007, **111**, 1248-1255.
41. P. K. Vemula, U. Aslam, V. A. Mallia and G. John, *Chem. Mater.*, 2007, **19**, 138-140.
42. S. P. Dubey, M. Lahtinen and M. Sillanpaa, *Colloids Surf., A*, 2010, **364**, 34-41.
43. T. Ishizaka, A. Ishigaki, H. Kawanami, A. Suzuki and T. M. Suzuki, *J. Colloid Interface Sci.*, 2012, **367**, 135-138.
44. S. P. Shukla, M. Roy, P. Mukherjee, A. K. Tyagi, T. Mukherjee and S. Adhikari, *J. Nanopart. Res.*, 2012, **14**, 981/981-981/911.
45. K. Kneipp, H. Kneipp, I. Itzkan, R. R. Dasari and M. S. Feld, *Chem. Rev. (Washington, D. C.)*, 1999, **99**, 2957-2975.
46. M. Bolboaca, T. Iliescu, C. Paizs, F. D. Irimie and W. Kiefer, *J. Phys. Chem. A*, 2003, **107**, 1811-1818.
47. B. Pergolese, M. Muniz-Miranda and A. Bigotto, *J. Phys. Chem. B*, 2004, **108**, 5698-5702.
48. N. Biswas, S. Thomas, S. Kapoor, A. Mishra, S. Wategaonkar, S. Venkateswaran and T. Mukherjee, *J. Phys. Chem. A*, 2006, **110**, 1805-1811.
49. Z. Yang, S. Si and Y. Fung, *Thin Solid Films*, 2007, **515**, 3344-3351.
50. J. R. Lakowicz, *Principles of Fluorescence Spectroscopy* 3rd edn., Springer, New York, 2006.
51. P. Manitto, D. Monti and E. Garbagnati, *Pediatr. Res.*, 1984, **18**, 378-381.
52. W. Patungwasa and J. H. Hodak, *Mater. Chem. Phys.*, 2008, **108**, 45-54.
53. Y. H. a. D.-H. Kim, *Langmuir*, 2011, **27**.
54. Q. Bian, J. Liu, J. Tian and Z. Hu, *Int. J. Biol. Macromol.*, 2004, **34**, 333-337.
55. W.-W. Bian, N. Zhang, F. Yan, S.-X. Wang and Y.-H. Li, *Fenxi Huaxue*, 2010, **38**, 1501-1504.
56. M. R. Eftink and C. A. Ghiron, *J. Phys. Chem.*, 1976, **80**, 486-493.
57. A. Ahmad, K. Kern and K. Balasubramanian, *ChemPhysChem*, 2009, **10**, 905-909.
58. D. L. Dexter, *J. Chem. Phys.*, 1953, **21**, 836-850.
59. M. K. Johansson and R. M. Cook, *Chem. - Eur. J.*, 2003, **9**, 3466-3471.
60. S. Franzen, J. C. W. Folmer, W. R. Glomm and R. O'Neal, *J. Phys. Chem. A*, 2002, **106**, 6533-6540.

61. B. Yang, R. C. Taylor, M. D. Morris, X. Wang, J. Wu, B. Yu, G. Xu and R. D. Soloway, *Spectrochim. Acta, Part A*, 1993, **49A**, 1735-1749.

62. Y. Z. Hsieh, N. S. Lee, R. S. Sheng and M. D. Morris, *Langmuir*, 1987, **3**, 1141-1146.

63. Z.-Y. Xiao and J.-H. Yin, *Anal Bioanal Chem*, 2013, **405**, 2723-2728.

64. S. Wang, H. Yao, S. Sato and K. Kimura, *J. Am. Chem. Soc.*, 2004, **126**, 7438-7439.

65. C. S. Weisbecker, M. V. Merritt and G. M. Whitesides, *Langmuir*, 1996, **12**, 3763-3772.

66. A. A. Volkert, V. Subramaniam and A. J. Haes, *Chem. Commun. (Cambridge, U. K.)*, 2011, **47**, 478-480.

67. D. V. Goia, *J. Mater. Chem.*, 2004, **14**, 451-458.

68. M. Zhou, B. Wang, Z. Rozynek, Z. Xie, J. O. Fossum, X. Yu and S. Raaen, *Nanotechnology*, 2009, **20**, 505606/505601-505606/505610.

69. H. Tsunoyama, N. Ichikuni, H. Sakurai and T. Tsukuda, *J. Am. Chem. Soc.*, 2009, **131**, 7086-7093.

70. J.-J. Max and C. Chapados, *J. Phys. Chem. A*, 2004, **108**, 3324-3337.

Table 1. FT-IR peaks of BR and AuBR powder

serial no.	bilirubin	Au-bilirubin (AuBR)	vibration mode
1	3406	3446	ν_{N-H}
2	3267	3446	ν_{N-H} (lactam)
3	3008	2995	ν_{N-H}
4	2912	2915	ν_{C-H}
5	2856	2854	ν_{N-H}
6	1695		$\nu_{C=O}$ (COOH)
7	1645	1647	$\nu_{C=O}$ (lactam)
8	1611		$\nu_{C=C}$
9	1568	1563, 1550	$\nu_{C=C}$
10	1499	1517	ring torsion
11	1445	1456	bridge carbon def, ring torsion
12	1406	1391	ν_{C-N}, CH_3 bending
13	1364, 1345		C-H bending (CH_3)
14	1300		bridge C-H bending, bridge $\nu_{C=C}$, ν_{C-N}
15	1250	1250	ring
16	1219	1219	ν_{C-C}
17	1188	1165	ring breathing
18	1108	1110	ν_{N-H}
20	989	1020	ring (C-N)

Figure caption

Figure 1: UV-vis spectra of bilirubin coated gold nanoparticles in different solution condition: (A) AuBR prepared at pH 9.0, washed with water and dispersed in milli-Q water at pH ~7 ; (B) AuBR prepared as above and stored for different days at 4 ^{o}C, re-suspended in milli-Q water just before the absorption measured; downward arrow indicated that the plasmon resonance band position was not changed and also indicated the age of the stored sample; (C) freshly prepared AuBR in the presence of different concentration of KCl solution and (D) AuBR suspension in the presence of different concentration of NaCl. The variation of the spectra in the presence of salt was very minimum and not individually marked. The vertical arrow indicated that the peak position was not much changed.

Figure 2: Transmission electron microscopic (TEM) image of bilirubin coated gold nanoparticles. The scale bar is shown in the bottom and it's 200 nm. The inset shows powder XRD diffraction pattern of AuBR nanoparticles. The peaks are assigned based on JCPDS Card no. 03-065-2870.

Figure 3: Changes in fluorescence spectra of bilirubin upon addition of different concentration of Au (III) in phosphate buffer, 5mM, pH 9.0 at room temperature. λ_{ex} = 470 nm and the path length of the cell was 10 mm. Both the excitation and emission slit widths were 5 nm. The lower panel shows S–V plot obtained using the fluorescence intensity at 520 nm and the presence of different concentration of Au (III).

Figure 4: Proposed structure of hydrogen bond stabilized bilirubin (A) and bilirubin attached to the gold nanoparticle (B).

Figure 5: FT-IR spectra of bilirubin powder (A) and AuBR (B) in solid state using KBr pellet. AuBR spectrum was broadened at high frequency region. In an inset in panel B is shown an expanded FT-IR spectrum of AuBR in the region 1000-1800cm^{-1}.

Figure 6: UV-Visible spectra of gold nanoparticles dispersed in 10 mM phosphate buffer solution at different pH and their color photograph. Nanoparticle solution was taken in disposable single sealed plastic cuvettes (Eppendorf) and placed on white surface before taking photograph under room light. The plasmon resonance peak positions in different pH conditions and the calculated size of the particles are also shown in the imbedded table.[52] The size was determined using the plasmon band and the database available at http://www.sigmaaldrich.com/materials-science/nanomaterials/gold-nanoparticles.html.